

Electronic Supplementary Information

Fouling behavior of polyethersulfone ultrafiltration membranes functionalized with sol-gel formed ZnO nanoparticles

Xin Li,^a Jiansheng Li,^{*a} Bart Van der Bruggen,^b Xiuyun Sun,^a Jinyou Shen,^a Weiqing Han^a and
Lianjun Wang^{*a}

^a *Key Laboratory of Jiangsu Province for Chemical Pollution Control and Resources Reuse, School of Environment and Biological Engineering, Nanjing University of Science and Technology, Nanjing 210094, China.*

^b *Department of Chemical Engineering, KU Leuven, W. de Croylaan 46, B-3001 Leuven, Belgium.*

Corresponding author. Tel/Fax: +86 25 84315351.

E-mail: lijsh@mail.njust.edu.cn; wanglj@mail.njust.edu.cn.

Experimental

Preparation of ZnO nanoparticles sol

Briefly, 2.75 g Zn (NO₃)₂·6H₂O and 0.6 g PVP were dissolved into 82.8 mL DMF to form a uniform solution under magnetic stirring for 30 min. Afterwards, the mixed solution was transferred into a 250 mL three-neck round-bottom flask and kept mechanical stirred for a further 20 min at 110 °C under refluxing condition. At this stage the colorless solution gradually turned to oyster white, indicating that the homogeneous ZnO nanoparticles sol in DMF was formed. The distributed situation and particle size of ZnO nanoparticles in DMF was analyzed using transmission electron microscopy (TEM, JEM-2100, JEOL, Japan).

Membrane characterization

The morphology of the membrane surface and the cross section was observed through a field emission scanning electron microscope (FE-SEM, FEI 250, Quanta). Before FE-SEM analysis, the membrane samples were dried with a supercritical drying apparatus (K850, EMITECH, Britain). The membrane cross sections were obtained by fracturing the membrane after immersing in liquid nitrogen. All the samples for FE-SEM were prepared by sputter coating a thin layer of platinum under vacuum to generate conductivity.

The pore size analysis of the prepared membrane was investigated by using a Capillary Flow Porometer (CFP Porolux 1000, IB-FT GmbH Berlin, German). The membranes were fully wetted with commercial low surface tension liquid Porefil (surface tension of 16 dyn cm⁻¹). The measurements consist of a wet-run program and a dry run program. The mean pore size r_m (nm) and maximum pore size r_{max} (nm) were determined with the aid of the computer software coupled to the CFP. The overall porosity (ε) was determined by the gravimetric method, as defined in the following equation ¹:

$$\varepsilon = \frac{\omega_1 - \omega_2}{A \times l \times d_w}$$

where ω_1 is the weight of the wet membrane (g); ω_2 is the weight of the dry membrane (g); d_w is the water density (0.998 g/cm³); l is the membrane thickness (cm) and A is the membrane area (cm²). The porosity is reported as the average of at least 5 measurements per membrane.

The surface roughness of the prepared membranes was analyzed by atomic force microscopy (AFM, Dimension Icon, Bruker, Germany). Approximately 1 cm² of the prepared membranes was

cut and glued on the glass substrate before being scanned ($5\ \mu\text{m} \times 5\ \mu\text{m}$). The mean surface roughness R_a , the root mean square of the Z data R_q and the mean difference between the five highest peaks and lowest valleys R_z were studied by AFM under the scanasyst. The average value of at least three random locations was reported to minimize the experimental error.

The surface composition of the membranes was determined using XPS, where samples of approximately $10\ \text{mm} \times 10\ \text{mm}$ were irradiated by soft X-rays.

Thermal investigations were carried out by TGA to study the behavior of the individual degradation steps of the pure and hybrid PES membranes. TGA at a heating rate of $10\ ^\circ\text{C}$ per minute under a flow of $100\ \text{mL}/\text{min}$ of nitrogen was used. Measurements were carried out for three pieces of a flat sheet membrane for every type of membrane with standard deviation below $\pm 0.2\%$ of weight loss.

The hydrophilicity of the membranes was examined by static contact angle measurement at $25\ ^\circ\text{C}$, using a drop shape analysis system (Krüss DSA30, Germany). A drop of $3\ \mu\text{m}$ deionized water was placed on the surface of membranes and then the contact angle between the water and membranes was measured. At least five measurements were made for each membrane and the averaged data are reported.

The selectivity of the fabricated membranes was evaluated through molecular weight cutoff (MWCO) analyses using a dead-end filtration system with a nitrogen gas cylinder. The system consisted of a filtration cell (FI-47, Zhejiang DD Water Industry Co., Ltd) and a solution reservoir with a volume capacity of $200\ \text{mL}$. Five different molar masses of polyethylene glycols (PEGs, $M_w=20, 100, 300, 600, 900\ \text{kDa}$) were used to characterize the MWCO of the membranes at $0.1\ \text{MPa}$. The test solution was prepared by mixing PEG in ultrapure water at the concentration of $1\ \text{g}/\text{L}$. For each filtration runs, the initial effluent collected for $15\ \text{min}$ was discarded to avoid interference from previous filtration runs. The concentration of samples from the feed and collected permeate were analyzed by means of total organic carbon (TOC) analysis (TOC-VCSH, Shimadzu, Japan) to determine solute rejection ($R=1-C_{\text{Permeate}}/C_{\text{Feed}}$). The MWCO of the membrane was determined as the lowest M_w where 90% PEG is retained. Membrane permeability and protein rejection were also measured; details of these procedures are described elsewhere ^{2, 3}. In order to verify the reproductivity of the obtained membranes, the repetitive experiments were conducted for five times at different areas of same type membranes.

Model foulants and synthetic foulant solutions.

According to the manufacturer, the molecular weight of the BSA was 67 kDa. SA has been widely used in membrane fouling research to represent polysaccharides that constitute a major fraction of soluble microbial products in wastewater effluent. According to the manufacturer, the alginate has a molecular weight in the range of 12-80 kDa. HA was obtained from Sigma-Aldrich (technical grade, St. Louis, MO). HA is a terrestrial peat-derived humic material, whose molecular weight values range from 4000 to 23000, and also been used extensively as a model organic foulant ^{2,4}

Evaluation of antifouling performance.

Prior to each filtration, the membrane was compacted with deionized water at 0.15 MPa for 10 min until the flux reached a plateau and then the pressure was lowered to the operating pressure of 0.1 MPa. The original membrane fluxes (J_0 with pure water and J_{S0} with the foulant-free solution) were measured (10 min each) first, then fouling was initiated by filtration with the foulant solution (Table S2 in ESI) for 0.5 h. After a 20 min period of recording the fouled-membrane fluxes (J_F with pure water and J_{SF} with the foulant-free solution, 10 min each), a ‘physical’ cleaning step (back wash in the dead-end filtration system with deionized water) was performed for 5 min. In the end, the water flux of the cleaned membrane (J_C with pure water and J_{SC} with the foulant-free solution) was measured again to determine the cleaning efficiency (η) ⁵, which was calculated as

$$\eta(\%) = \frac{J_{SC} - J_{SF}}{J_{S0} - J_{SF}} \times 100$$

The filtration experiments with different kinds of foulants have been repeated for five times to show the re-productivity of the obtained membranes.

In order to further assess the long-term fouling reversibility of the resultant membranes, three sequential cycles of dead-end filtration were carried out with mixture synthetic solutions. After 10 min of recording the pure water flux (J_0), filtration with a synthetic mixture was carried out for 1 h at 0.1 MPa. Afterwards the membrane was back flushed with deionized water for ‘physical’ cleaning, and the flux of the cleaned membrane was measured with pure water (J_C) at the end of one filtration cycle. The flux recovery (R) after ‘physical’ cleaning in each filtration cycle was calculated as

$$R_i(\%) = \frac{J_{Ci} - J_{Fi}}{J_{S0} - J_{SF}} \times 100$$

where J_{Fi} is the fouled-membrane flux at the end of fouling and J_{Ci} is the pure water flux of the cleaned membrane in the i th filtration cycle. All experiments were carried out at room temperature.

Results and discussion

Morphology and structure of PES hybrid membrane.

AFM was used to examine the surface roughness of the membranes in this study. The $5\ \mu\text{m}\times 5\ \mu\text{m}$ three-dimensional AFM images and the average roughness of the resultant membranes are shown in Fig. S3 and Table S3, respectively. In these images, the brightest area represents the highest point of the membrane surface and the dark regions indicate valleys or membrane pores. The mean roughness (R_a) decreased with the increase of the amount of ZnO nanoparticles, from 5.9 nm for the neat PES membrane to 4.0 nm for the PES-0.75 membrane. It is hypothesized that the introduction of more ZnO nanoparticles had a tendency to cover the concavities of the composite membrane surface. These results were consistent with qualitative FE-SEM observations (Fig. 1 in text). The reduced surface roughness of the membrane after the addition of ZnO nanoparticles could have a profound effect on the fouling tendency of the membranes, as will be discussed in the text.

To uncover the composition of the samples, XPS was employed to probe surface properties of the ZnO/PES hybrid membrane. As shown in Fig. S4(A), the PES-0.75 membrane is mainly composed of four elements, that is, C1s, O1s, S2s/S2p and Zn2p. Noticeably, featured peaks with binding energy of 1020.8 eV in core-level spectrum of Zn agree with the chemical elemental state of Zn^{2+} (ZnO)⁶. The XPS spectra demonstrate that ZnO is successfully introduced in PES hybrid membranes. The presence of ZnO nanoparticles was also investigated by TGA (Fig. S5). The TGA curves show that the decomposition temperature for the selected membrane was around 420 °C. This result is coherent with reported values in the literature⁷. A small increase was observed for the residual weight at temperatures above 650 °C, as a result of the addition of ZnO nanoparticles. Considering that the residual weight obtained for the control membrane should be related to the organic content of PES, the difference between the percentages of the pure PES membrane and the ZnO/PES membrane should correspond to the ZnO fraction⁸. This further confirms the presence of ZnO nanoparticles in the PES hybrid membrane composition.

The surface hydrophilicity of the neat and composite membrane was confirmed by static water contact angle measurements, as shown in Table 1. The neat PES membrane has a high contact angle of 75.5°, corresponding to the relatively hydrophobic nature of polymeric matrix. When ZnO

nanoparticles were added into PES membrane, the contact angles gradually decreased to 62.6° for the PES-0.75 membrane, which means that the addition of ZnO nanoparticles has enhanced the membrane hydrophilicity. As discussed in the text, the porosity of composite membrane increased with the addition of ZnO nanoparticles due to the acceleration of the demixing process. Considering that more smooth surfaces were obtained, as evidenced by AFM data, the water droplet would more easily spread on the surface of composite membrane. Furthermore, ZnO nanoparticles enhanced the wettability of internal pore channels and further improved the hydrophilicity of the PES membrane. As a result, the ZnO/PES membranes have a smaller contact angle than the neat membranes.

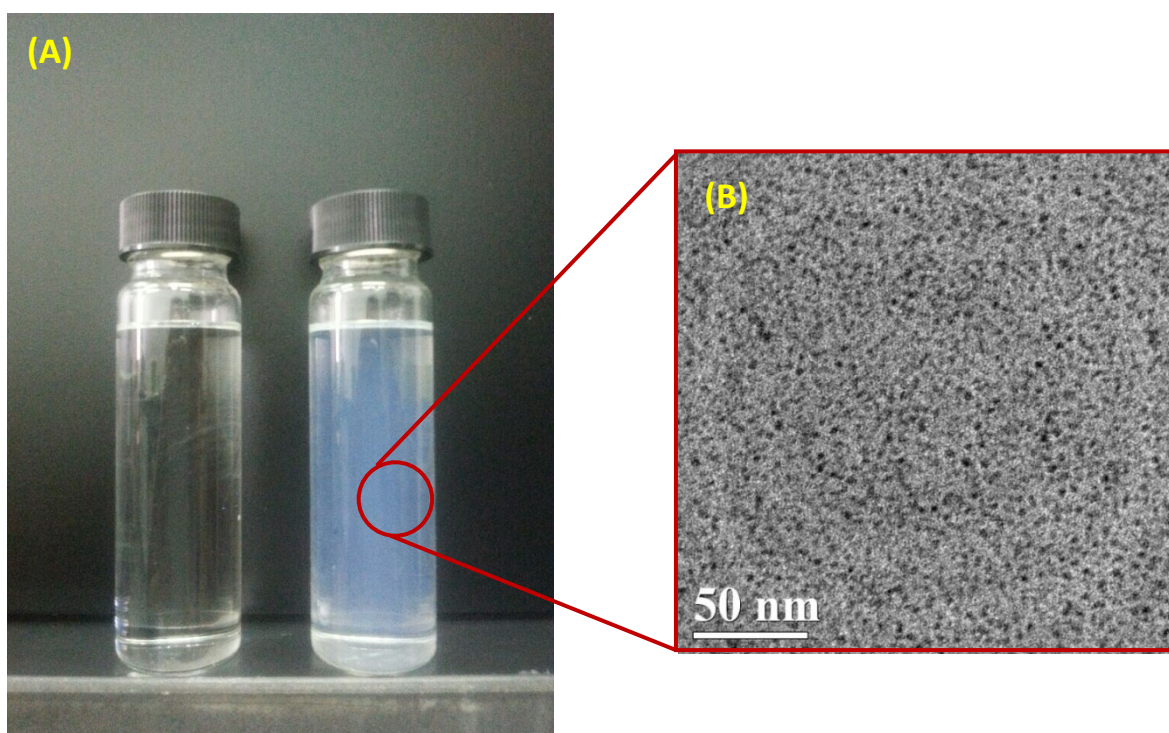
Filtration performance.

The membrane separation can also be investigated by building the rejection curves which plot the rejection values vs. molar mass. As shown in Fig. S6, The rejection curve of pure PES membrane is steeper than that of hybrid membranes and a 90% retention was measured as 255 kDa (i.e., MWCO of 255 kDa), indicating a smaller membrane pore size. However, with the increase of the amount of ZnO nanoparticles in PES membranes, the curve has a gradual trend with the MWCO of hybrid membranes increasing from 267 kDa for the PES-0.25 membrane to 300 kDa for the PES-0.75 membrane. These results are mainly attributed to the relatively large pore size and high pore porosity which have been discussed above. The variation of the MWCO of pure and hybrid membranes is in accordance with the results of BSA rejection (Fig. 2 in text).

References

1. J. María Arsuaga, A. Sotto, G. del Rosario, A. Martínez, S. Molina, S. B. Teli and J. de Abajo, *J. Membr. Sci.*, 2013, 428, 131-141.
2. X. Li, X. Fang, R. Pang, J. Li, X. Sun, J. Shen, W. Han and L. Wang, *J. Membr. Sci.*, 2014, 467, 226-235.
3. X. Fang, J. Li, X. Li, X. Sun, J. Shen, W. Han and L. Wang, *J. Membr. Sci.*, 2015, 476, 216-223.
4. K. Katsoufidou, S. Yiantsios and A. Karabelas, *J. Membr. Sci.*, 2005, 266, 40-50.
5. Y. Mo, A. Tiraferri, N. Y. Yip, A. Adout, X. Huang and M. Elimelech, *Environ. Sci. Technol.*, 2012, 46, 13253-13261.
6. F.-X. Xiao, *ACS Appl. Mater. Inter.*, 2012, 4, 7054-7062.
7. A. Sotto, A. Boromand, S. Balta, J. Kim and B. Van der Bruggen, *J. Mater. Chem.*, 2011, 21, 10311-10320.
8. A. Sotto, A. Boromand, R. Zhang, P. Luis, J. M. Arsuaga, J. Kim and B. Van der Bruggen, *J.*

Colloid Interf. Sci., 2011, 363, 540-550.



articles

Fig. S1. (A) Photographs of Zn²⁺/DMF solution and ZnO nanoparticles sol; (B) TEM image of ZnO

nanoparticles sol.

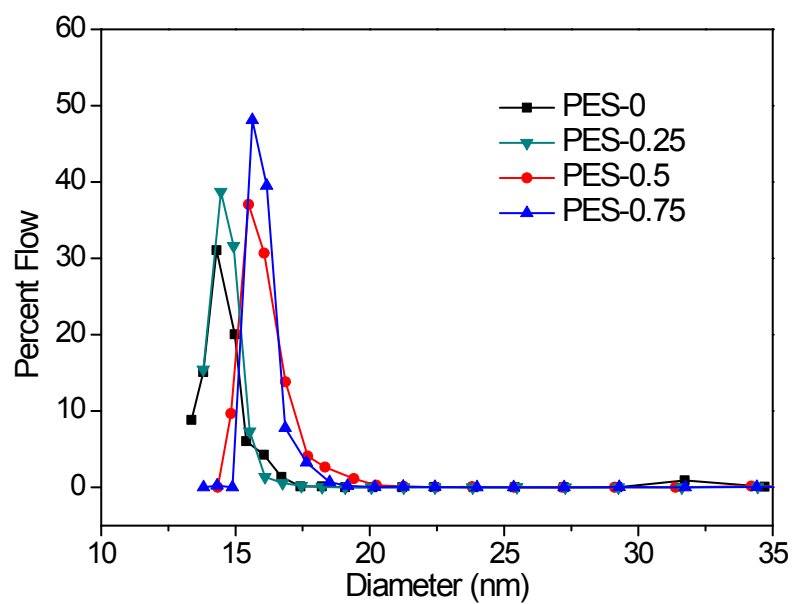


Fig. S2. Pore size distribution of the pure and hybrid PES membranes.

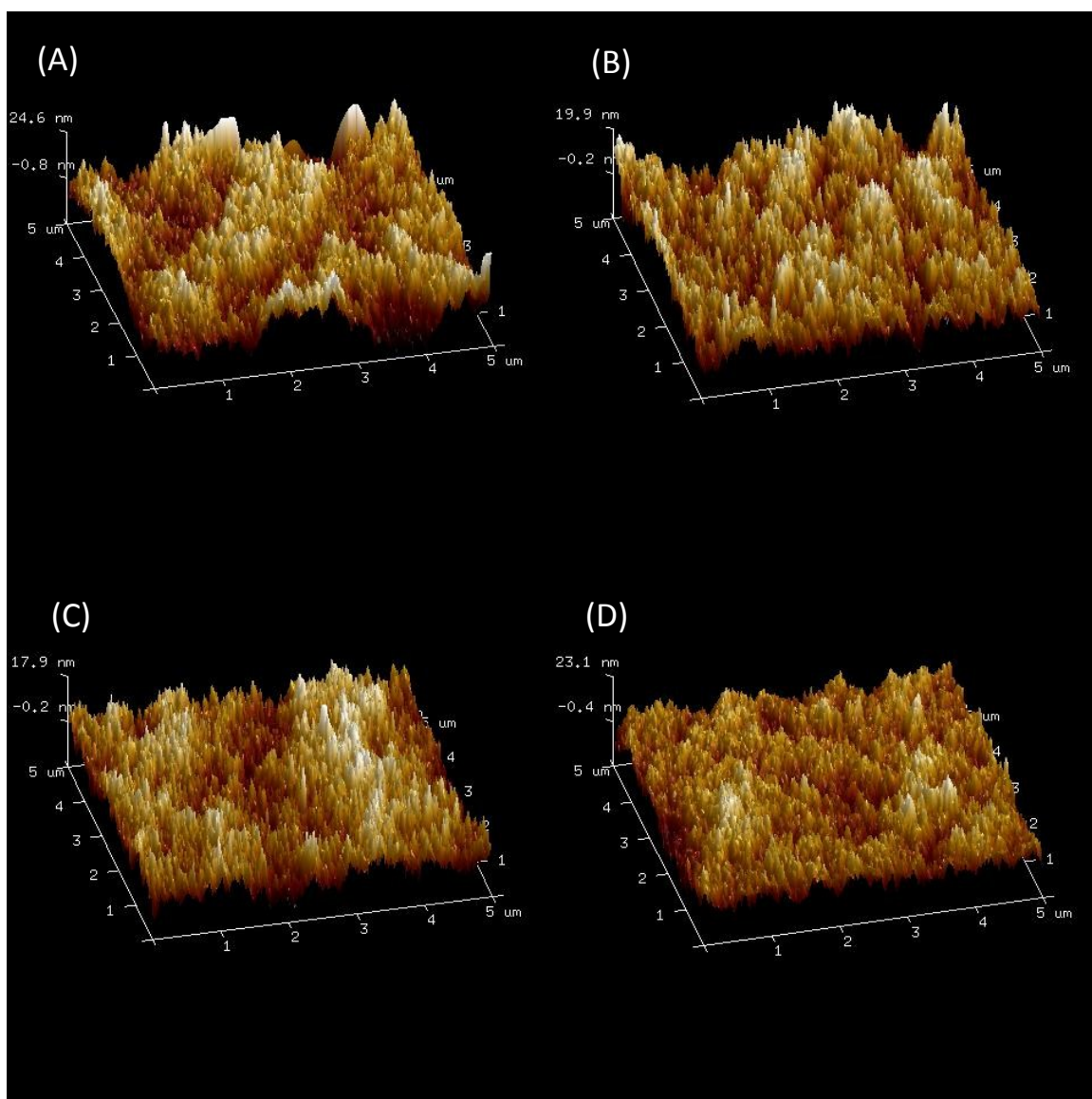


Fig. S3. Three dimensional AFM images for (A) PES-0, (B) PES-0.25, (C) PES-0.5, (D) PES-0.75.

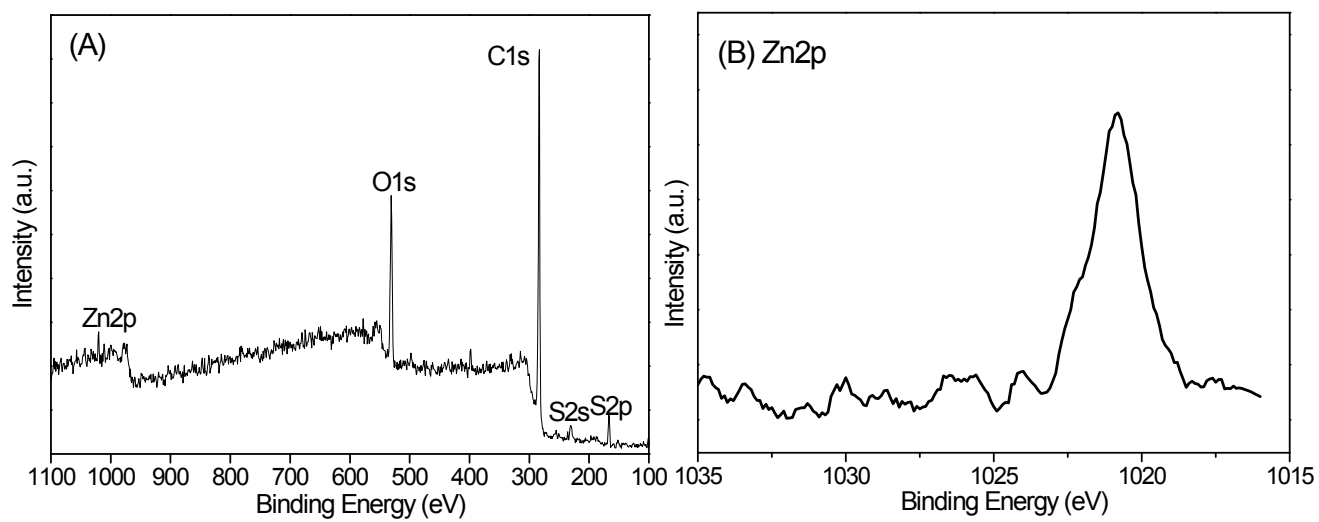


Fig. S4. (A) Survey and high-resolution XPS spectra of (B) Zn 2p for PES-0.75 membrane.

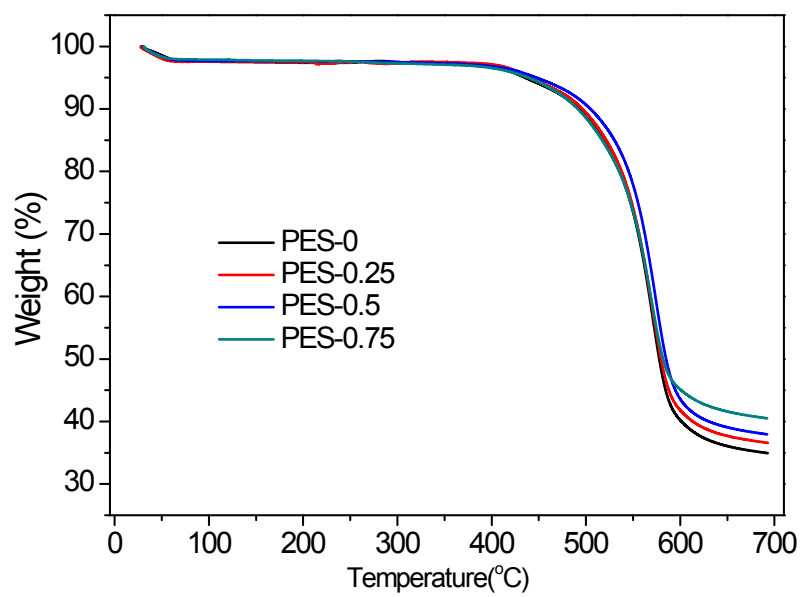


Fig. S5. TGA curves of PES-0, PES-0.25, PES-0.5, PES-0.75.

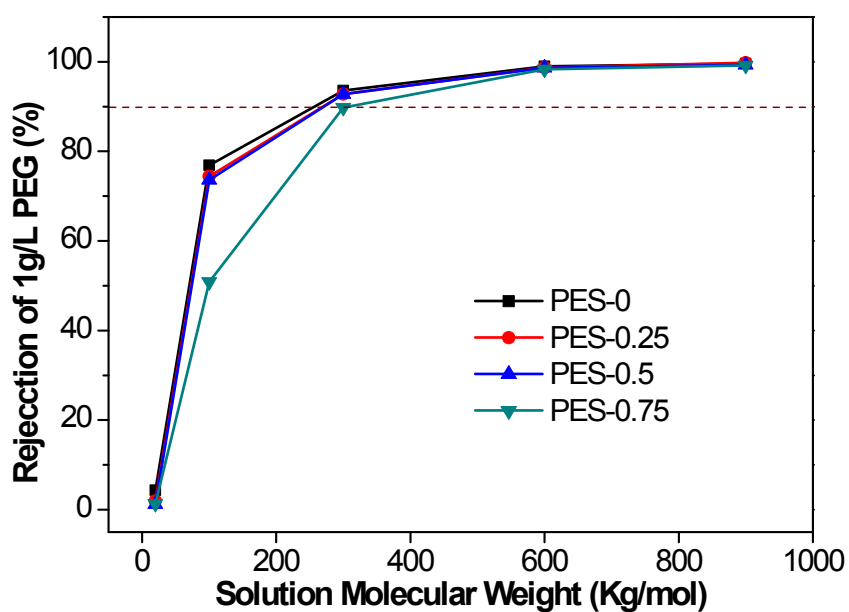


Fig. S6. Molecular weight cutoff (MWCO) of the pure and hybrid membranes. The dashed line (at 90% rejection) indicated the MWCO of the examined membranes.

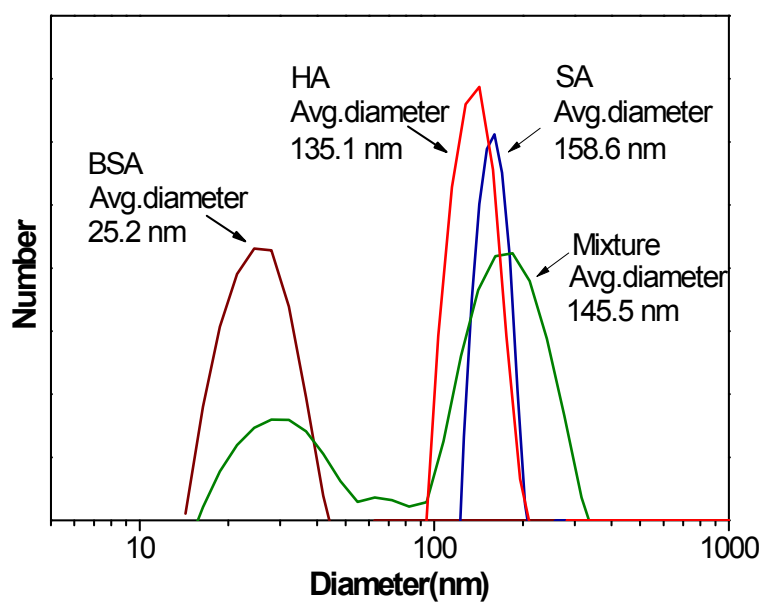


Fig. S7. Size distribution of the model organic foulants in the corresponding synthetic solutions (Table S2). Also presented are the average diameters.

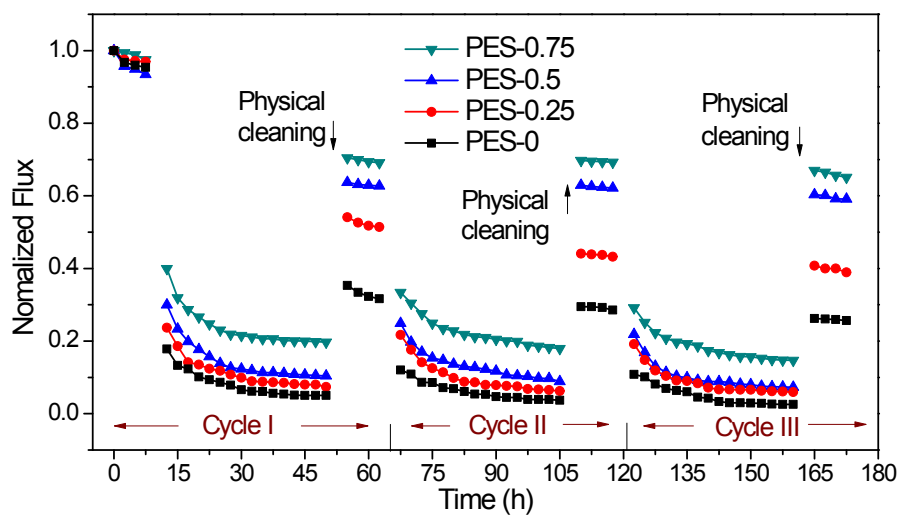


Fig. S8. Flux decline of different membranes in three filtration cycles using the dead-end system filtering mixture foulant solutions.

Table S1 Compositions of casting solution used in this study

	PVP(g)	PES(g)	Zn (NO ₃) ₂ ·6H ₂ O(g)	DMF(mL)
PES-0	4	15	0	85.70
PES-0.25	4	15	0.92	84.75
PES-0.5	4	15	1.83	83.78
PES-0.75	4	15	2.75	82.80

Table S2 Chemistry of different foulant solutions used for filtration tests

Items		Different solutions				
		Mixture	SA	HA	BSA	Foulant free
Model foulant (mg/L)	SA	30	30	—	—	—
	HA	20	—	20	—	—
	BSA	15	—	—	15	—
Inorganic Components (mM)	CaCl ₂	2	2	2	2	2
	MgCl ₂	1	1	1	1	1
	NaHCO ₃	2	2	2	2	2
	NaCl	10	10	10	10	10

Table S3 AFM surface roughness values of the neat and hybrid membranes.

	Surface	Roughness		
	area(μm^2)	$R_a(\text{nm})$	$R_q(\text{nm})$	$R_z(\text{nm})$
PES-0	25.5 \pm 0.5	5.85 \pm 1.16	7.32 \pm 1.21	61.2 \pm 6.1
PES-0.25	25.4 \pm 0.3	4.57 \pm 1.02	5.74 \pm 0.96	54.5 \pm 4.6
PES-0.5	25.4 \pm 0.2	4.17 \pm 0.86	5.22 \pm 0.68	52.9 \pm 4.5
PES-0.75	25.4 \pm 0.6	4.00 \pm 0.92	5.04 \pm 0.54	43.2 \pm 3.7